Mechanisms of Low-Temperature Diffusion Saturation of Structural Steel with Nitrogen in the Plasma of a Low-Pressure Arc Discharge

I.M. Goncharenko, S.V. Grigoriev, Yu.F Ivanov, Yu.A. Kolubaeva*, N.N. Koval, P.M. Schanin, Yang Si-Ze**

Institute of High-Current Electronics, SB, RAS, 4 Akademichesky Ave., Tomsk, 634055, Russia,
Phone: (+3822)491300, Fax: (+3822)492410, E-mail: potter@opee.hcei.tsc.ru
** Tomsk State University, Tomsk, 634050, Russia*
*** Institute of Physics Chinese Academy of Sciences, Beijing, KNR*

Abstract – The structure and the phase composition of the diffusion saturation zone of 40Cr- and 12Cr2Ni4N-type steels subjected to nitriding in the plasma of a low-pressure gas discharge have been studied by the methods of optical, scanning, and diffraction electron microscopy. An essential potentialities have been revealed to nitride steel at low (~200 °C) temperatures. The structural-phase state of the nitrided layer has been shown to depend strongly on the morphology and phase composition of the initial material.

1. Introduction

Ion nitriding in the plasma of a gas discharge, as a rule, is realized in the nitrogen-hydrogen atmosphere at elevated temperatures (~500–520 °C) [1]. Introduction of hydrogen is required to fix oxygen present in the discharge chamber at a high gas pressure and forming an oxide film at the steel surface that substantially reduces the nitriding rate. The treated specimen is heated to increase its diffusion saturation rate. When nitriding in a low-pressure discharge, it is possible to minimize the role of hydrogen in the nitrogen-hydrogen atmosphere [2] or exclude it completely [3]. In [3] it is shown that 40Cr steel specimens can be nitrided in a low-pressure arc discharge ($\sim 10^{-1}$ Pa) without introducing hydrogen if a negative bias voltage of the order of several hundreds of volts is applied to the treated article. The oxide film, which impedes the nitrogen supply into the specimen volume, is destroyed due to bombardment of the surface by N ions accelerated in the near-wall layer of the space charge. The nitride coating formed by this method of nitriding is examined in detail elsewhere [4].

In this work we analyzed the results of studies of the structural-phase state of a steel volume located immediately under the nitride layer, i.e., a so-called diffusion saturation zone.

2. Materials and Experimental Procedure

The test material was 40Cr-type steel (0.4% C; 1.0% Cr) and 12Cr2Ni4 (0.14%C, 2.3%Cr%, 3.8%Ni) in the ferrite-pearlite and martensite states. The specimens had the form of cylinders of diameter 20 mm and height 10 mm. To form the ferrite-pearlite structure the specimens were annealed at a temperature of 860 °C for 1.5 h with subsequent air cooling. The martensite structure was obtained by water hardening of the specimens from a temperature 850 °C for 2.5 h. Diffusion saturation of steel with nitrogen was realized in the plasma of a low-pressure vacuum arc discharge for 2 h at an average specimen temperature of ~200 °C (40Cr steel) and 530 °C (12Cr2Ni4 steel). The procedure of preparing and saturating the specimens with nitrogen is described in detail in [3, 5]. The structure and the phase state of the materials were examined by the methods of thin-foil diffraction microscopy with the use of an TEM-125 device. We analyzed the material volume immediately under the nitride layer and that ~3–5 μm away from it (the nitride layer was removed by electrolytic thinning).

3. Results and Discussion

Nitriding at a temperature of 200 °C even for 2 h involves considerable changes of the structural-phase state of hardened and normalized steels. In hardened steel the transformation of the defect substructure lies in a substantial (up to $\sim 7 \cdot 10^{10}$ cm^{-2}) decrease in scalar dislocation density, in the formation of subgrains (centers) of dynamic recrystallization along the grain boundaries and at their junctions, in coalescence of the martensite crystal boundaries grouped in laths, and finally, in the formation of crack-containing submicrocrystalline α-phase regions near the grain boundaries, which are characterized by a high level of bend-torsion of the crystalline lattice. The change of the phase state is governed by the structural-phase state of an initial material. In the lath martensite regions of $Fe_4(Fe(CN)_6)_3$ iron carbonitride appears along the crystal boundaries and at the crystal junctions (Fig. 1). In lamellae of the low-temperature martensite iron nitride nanoparticles of composition $Fe_{16}N_2$ are formed on dislocations. Along the boundaries of dynamic recrystallization centers γ-Fe_4N–type nanoparticles are distinguished. In crystals of the high-temperature lamellar martensite iron carbonitride nanoparticles of nonstoichiometric composition are formed.

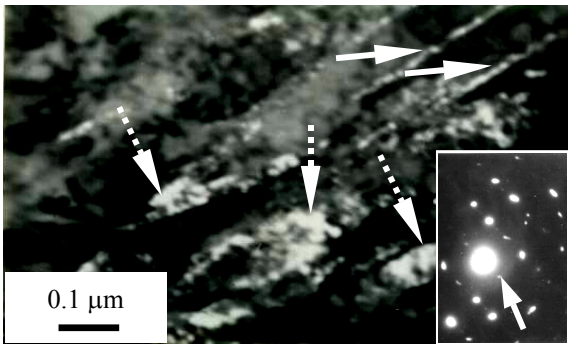

Fig. 1. Dark-field image of iron carbide particles (indicated by solid arrows) and iron carbonitride particles (indicated by dotted arrows) obtained in coincident reflex [020]Fe_3C + +[110]$Fe_4(Fe(CN)_6)_3$. the inset shows an electron-diffraction pattern (the dark-field reflex is indicated by the arrow)

In normalized steel a substructure in the form of dislocation pileups in {110}α-Fe-type directions is observed in free ferrite grains. The dislocation lines are decorated by iron nitride particles of compositions γ-Fe_4N and $Fe_{2-3}N$. The particles are round in shape and their average size varies in the range from 10 to 20 nm. In terms of morphology a similar structure is formed in ferrite interlayers of lamellar martensite grains, too. Namely, parallel rows of iron nitride nanoparticles of composition $Fe_{2-3}N$, are observed along directions of the type {110}α-Fe (Fig. 2).

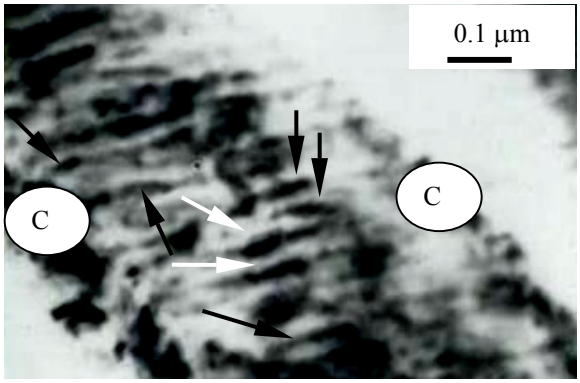

Fig. 2. TEM image of the lamellar pearlite substructure. Iron nitride particles of composition $Fe_{2-3}N$ are indicated by arrows, C – Fe_3C lamellae

The distance between the rows is ~25–40 nm and the average particle size is ~20 nm. In [6] such structures in the form of bands of periodically varying contrast were observed in the ferrite component of a perlite colony on short-run annealing of carbon steel of Fe-0.8%C. Their emergence was due to the periodically varying elastic stress field present in ferrite lamellae. At the same time, in the process of nitriding fragmentation of cementite lamellae and the formation of $Fe_{20}C_9$ and Fe_2C carbide particles inside them are observed. Modification of the globular pearlite is inessential and manifests itself only in some increase in the scalar density of dislocations forming the substructure.

Diffusion saturation of steel (we analyzed the Fe-0.14%C–2.3%Cr%–3.8%Ni steel structure) at a temperature of 530 °C led to more drastic changes of the state of the defect substructure and phase composition of the specimens, as compared to those considered above (Fe–0.4%C–1%Cr steel).

In the hardened steel specimens the transformation of the defect substructure is in a considerable decrease in scalar dislocation density (from $10 \cdot 10^{10}$ to $3.5 \cdot 10^{10}$ cm^{-2}), in fragmentation of martensite crystals, and in destruction of the intralath structure. Laths formed by martensite crystals whose cross-sectional dimensions are three-four times larger than those of the lath martensite in the initial state are observed. The last fact indicates that the boundaries of three-four adjacent crystals becomes scattered, thus forming a coarse-grained (block) lath. The volume fraction of such laths makes up ~50% of the martensite structure. Thus, in the hardened steel specimens in question laths of two types – with and without block structure are formed. In the first case, a lath consists of blocks of martensite crystals separated by small-angle boundaries; the boundaries between the blocks are large-angled. In the second case, the martensite crystals, which from a lath, have large-angle misorientations. On heating (in the process of nitriding) the small-angle boundaries separating crystals within a block are first to be broken and then the large-angle boundaries separating the blocks. Note that the block structure of laths was observed earlier in carbon-free Fe-(15–25)%Ni and low-carbon Fe-(0.15–0.20)%C steels [7, 8]. Nitriding of steel gives rise to the initial stages of recrystallization of the material layer in question. Recrystallization centers (subgrains) appear along the grain boundaries, at their junctions and at the junctions of martensite laths. In the majority of cases subgrains are round in shape and their sizes vary in the range from 0.25 to 1.1 μm. The volume fraction of subgrains is comparatively small (~5% of the structure of the given layer). The changes of the defect substructure of the steel layer under study are accompanied by the formation of iron nitride particles of composition ε-Fe_2N. The particles are formed exclusively along the intraphase boundaries – boundaries of grains, laths, martensite crystals and subgrains (Fig. 3).

At a distance of 3–5 μm from the nitride layer the martensite lath structure fails almost completely – the volume fraction of laths whose morphology is similar to that of laths in the initial state is ~14% of the steel structure. The prevailing component of the steel substructure is made up of grains and subgrains of recrystallization whose volume fraction reaches ~45 % of the material and the rest part is formed by block laths. Extended intermediate layers of the $Fe_4(Fe(CN)_6)_3$ phase which, in particular cases, is combined with ε-Fe_2N-phase particles are formed along the martensite crystal boundaries.

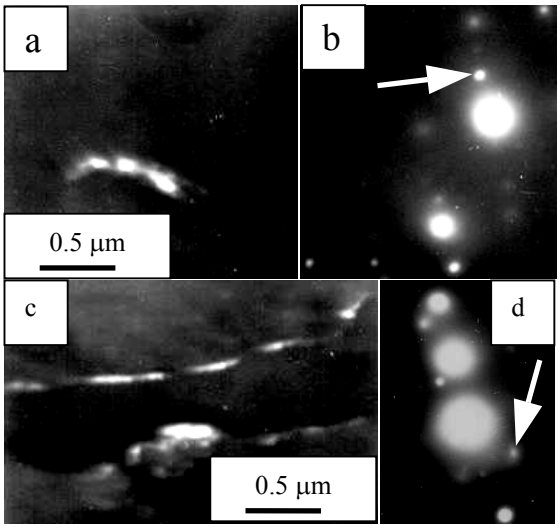

Fig. 3. TEM image of iron nitride particles formed immediately under the nitride layer (prehardened state). a, c – dark-fields obtained in [110]ε-Fe_2N and [111]ξ-Fe_2N reflexes; b, d – electron-diffraction patterns for (a) and (c), respectively (the dark field reflexes are indicated by arrows)

Nitriding of normalized steel above all else caused complete rearrangement of the defect substructure of the material volume immediately adjacent to the nitride layer (foil of thickness ~0.2 μm). First, in the grain volume of the lamellar pearlite a ferrite-based subgrain structure is formed where the average subgrain size is ~0.2 μm. Globular cementite particles are arranged along the subgrain boundaries and inside the subgrains a dislocation substructure with a scalar dislocation density of $\sim 2.7 \cdot 10^{10}$ cm^{-2} is observed. Second, in the volume of ferrite grains a structure with a high density of bend extinction contours is formed that is testimony to a high level of the bend-torsion amplitude of the crystalline lattice. These regions are also two-phase regions: α-Fe and γ-Fe_4N reflexes are revealed on electron-diffraction patterns. Consequently, diffusion saturation of ferrite-pearlite steel with the formation of a nitride layer ensures a rather high level of deformation of the subsurface material layer. This deformation initiates recrystallization and is accompanied by the formation of regions with a high level of bend-torsion of the crystalline lattice. This layer is thin. At a distance of ~0.5–1.0 μm from the nitride layer a structure formed by ferrite grains and lamellar pearlite colonies is observed. A peculiarity of this structure is a slightly increased scalar density of dislocations located in ferrite grains ($\sim 3.8 \cdot 10^{10}$ cm^{-2}), the presence of regions with a subgrain structure in some cases, and iron nitride nanoparticles of composition γ-Fe_4N. In going deep into the material to a distance of ~5 μm a structure which is much the same as that of the initial state is revealed, i.e., the structure consisting of pearlite grains and structurally free ferrites grains.

4. Conclusion

In these studies it has been ascertained that diffusion saturation with nitrogen at a temperature of 550 °C (12Cr2Ni4N steel) occurs under the action of at least three concurrently acting factors – force, temperature and concentration factors. The first fact assists in elastoplastic deformation of the material, the second one leads to relaxation of the defect substructure, and the third factor stabilizes the substructure formed in the material by changing the state of the solid solution of the matrix and by forming atmospheres and segregations and also nitride and carbonitride phase particles which are predominantly located on crystalline defects. In the volume immediately under the nitride layer the first and second factors prevail. In going from the nitriding surface deep to the specimen the effect of the first factor is weakened, the action of the second remains nearly unchanged, and that of the third factor gradually decreases. The degree to which these factors show themselves up is governed by the structural-phase state of the initial material

Thus, nitriding of steel at a temperature of 500–550 °C makes impossible the use of materials with a structurally instable state of the crystalline lattice (submicro- and nanocrystalline materials, prehardened steels, etc.). The estimates we have made show that nitriding in low-pressure gas discharges can be realized to advantage at much lower temperatures. Actually, at a gas pressure $p = \sim 9 \cdot 10^{-1}$ Pa and plasma ion density $n = 2 \cdot 10^9$ cm^{-3}, the free path of an ion in its proper gas $\lambda = 0.7$ cm. At a bias potential $U = -200$ V this is comparable with the width of the near-wall layer of the space charge $L = 0.6$ cm determined from the equality of the current density from the plasma and the ion current density in the acceleration gap calculated from the "3/2" (Child-Longmuir) law:

$$L = \frac{2}{3}\sqrt{\frac{\varepsilon_0}{0.4 n_e}} \cdot \sqrt[4]{\frac{U_c^3}{ekT_e}},$$

where ε_0 is the dielectric constant, n is the plasma density, e is the unit charge, k is Boltzmann's constant, T_e is the temperature of an electron, U is the bias voltage. Thus, the oxide film which impedes nitrogen supply into the specimen volume will be destroyed due to bombardment of the surface by N ions accelerated in the near-wall layer of the space charge.

These conclusions have found complete support in studying the structural-phase state of 40Cr-type steel nitrided at a temperature 200 °C. Comparison of the data obtained in examining the diffusion saturation layer of 40Cr steel in the prehardened and normalized states makes it possible to point out the following. First, no dynamic recrystallization centers are present in the ferrite-pearlite structure that is governed by the substantially lower crystalline defect density in the given material, as compared to steel hardened to

martensite. And second, it is the more developed processes of phase formation which are in the formation of nitrides with high relative density of N atoms in ferrite-pearlite steel counting upon a Fe atom. It is likely that the last fact is also governed by the difference in the defect substructure of ferrite-pearlite and martensite steels. It is known that structural defects of steel may accumulate on themselves up to 0.2–0.25 at % of interstitial impurity in the form of segregations at the intraphase and interphase boundaries and Cottrell and Suzuki atmospheres near dislocations and also in dislocation cores [9, 10]. It is fixing of N atoms by the defect substructure of martensite steel that leads to a delay of phase transformations, as compared to ferrite-pearlite steel.

References

[1] B.N. Arzamasov, A.G. Bratukhin, Yu.S. Eliseev, T.A. Panaiotty, *Chemicothermal ion treatment of alloys*, Moscow, MSTU Press, 1999, 400 pp.

[2] S. Parancandola, O. Kruse, W. Moller, J. Appl. Phys. Lett. **75**, No. 13, 185 (1999).

[3] P.M. Schanin, N.N. Koval, I.M. Goncharenko, S.V. Grigoriev, Physics and chemistry of material treatment, No. 3, 16 (2001).

[4] A.D. Korotaev, S.V. Ovchinnikov, A.N. Tyumentsev, Physics and chemistry of material treatment, No. 3, 16 (2004).

[5] L.G. Vintizenko, S.V. Grogoriev, N.N. Koval, V.S. Tolkachev, I.V. Lopatin, P.M. Schanin, Izv. Vyssh. Ucheb. Zaved. Fizika, No. 9, 28 (2001).

[6] I.L. Yakovleva, L.E. Karkina, Yu.V. Khlebnikova, V.M. Schastlivtsev, D.A. Mirzaev, Physics of metals and physical metallurgy, **94**, No. 5, 67 (2002).

[7] T. Maki, K. Tsuzaki, I. Tamyra, Trans. Iron and Steel Inst. Japan **20**. No. 4, 207 (1980).

[8] I.M. Marder, A.R. Marder, Trans. ASM **62,** No. 1, 1 (1969).

[9] V.G. Kurdyumov, L.M. Utevskii, R.I. Entin, Transformations in iron and steel, Moscow, Nauka, 1977, 236 p.

[10] V.K. Babich, Yu.P. Gul, I.E. Dolzhenkov, *Strain aging of steel*, Moscow, Metallurgia, 1972, 320 pp.